NUMERICAL ANALYSIS OF HARDWOOD TIMBER BEAMS REINFORCED WITH STEEL PLATE SCREWED

Pedro Ignácio Lima Gadêlha Jardim[2*], Fernando Júnior Resende Mascarenhas[3], Diego Henrique de Almeida[4], Francisco Antonio Rocco Lahr[5] and André Luis Christoforo[6]

[1] Received on 14.02.2022 accepted for publication on 25.04.2022.
[2] Universidade Federal de Rondônia, Departamento de Engenharia Civil, Porto Velho, RO - Brasil. E-mail: <eng.pedrojardim@gmail.com>.
[3] Universidade de Coimbra, Programa de Pós-Graduação em Engehnaria Civil, Coimbra, UC - Portugal. E-mail: <fer.jr.resende@hotmail.com>.
[4] Universidade Federal de Rondônia, Departamento de Engenharia Civil, Porto Velho, RO - Brasil. E-mail: <diegoalmeida@unir.br>.
[5] Universidade de São Paulo, Departamento de Engenharia de Estruturas, São Carlos, SP - Brasil. E-mail: <frocco@sc.usp.br>.
[6] Universidade Federal de São Carlos, Departamento de Engenharia Civil, São Carlos, SP - Brasil. E-mail: <alchristoforo@ufscar.br>.
*Corresponding author.

ABSTRACT – There are several technologies to recover and strengthen timber structures. Two usual alternatives are: the use of steel plates screwed and carbon fiber mats glued with epoxy adhesive. A gap was observed in the literature regarding the study of reinforcement in hardwood timber beams with cross-section loss, commonly found in attacks by biotic or abiotic agents. This study aimed to analyze the flexural stiffness recovery capacity of steel plate screwed to a timber beam with different cross-sectional losses, with a special interest in the effect caused by different bolt arrangements. The results were compared with simulations made using a carbon fiber mat (CF). It was possible to observe that, despite presenting lower efficiency than the CD, the use of steel plate screwed could return the initial stiffness in some models, and the specification of the bolts is relevant in obtaining the results.

Keywords: Composite materials; structural recovery; composite structures.

ANÁLISE NUMÉRICA DE VIGAS DE MADEIRA FOLHOSA REFORÇADAS COM CHAPA DE AÇO PARAFUSADA

RESUMO – Existem diversas tecnologias para recuperar e reforçar estruturas de madeira. Duas alternativas usuais são: a utilização de chapas de aço parafusadas e a utilização de mantas de fibra de carbono coladas com adesivo epóxi. Foi observado uma lacuna na literatura quanto ao estudo de reforço em vigas de madeira com perda de seção transversal, comumente encontrado em ataques de agentes bióticos ou abióticos. O objetivo desse estudo foi analisar a capacidade de recuperação da rigidez à flexão da chapa de aço parafusada em uma viga de madeira folhosa com diferentes perdas de seção transversal, com especial interesse no efeito provocado por diferentes arranjos de parafusos. Os resultados foram comparados com simulações feitas utilizando manta de fibra de carbono (FC). Foi possível observar que, apesar de apresentar eficiência inferior à FC, a utilização da chapa de aço parafusada teve capacidade de retornar a rigidez inicial em alguns modelos e a especificação dos parafusos possui relevância na obtenção dos resultados.

Palavras-Chave: Materiais compósitos; recuperação estrutural; estruturas mistas.

1. INTRODUCTION

Some studies were dedicated to the survey of pathological manifestations in timber structures, being commonly found loss of cross-section in the elements of the structure due to the decay process of the wood, usually associated with excess moisture and attack by biotic agents (Guevara et al., 2019; Martins e Fioriti, 2016).

There are several technologies for reinforcing and recovering wood (Guevara et al., 2019; Martins e Fioriti, 2016; Schober et al., 2015); for example, the use of plates or mats of various composites such as carbon fiber or glass, usually fixed to the structure with specific adhesives. According to Lukin et al. (2021), in elements subjected to bending, this type of reinforcement must be fixed in tensioned regions with greater deformations, being called rational reinforcement.

A solution for reinforcing deteriorated wood parts using the most common materials in civil construction is applying a steel plate screwed to the element. One technique for using steel plates on timber beams is gluing them with epoxy adhesive or similar material that guarantees a high degree of adhesion between the wood and the steel. However, the procedure is challenging to execute and control when carried out in loco (Burdzik e Skorpen, 2016). An alternative is to use mechanical fastening devices, such as nails and screws, to solidify the materials acting on the structural element. In the studies by Burdzik e Skorpen (2016), it was identified that stiffness of the set increases as the spacing of the mechanical fasteners decreases, and the stiffness of the timber is preponderant in the modulus of elasticity of the set.

The behavior of the timber-steel composite element is directly associated with the ability of mechanical fasteners to transmit forces. In the studies by Waseem et al. (2022), it was verified that the stiffness of the timber-steel assembly increases when the spacing of the mechanical fasteners is smaller. Currently, there is a gap in the studies of applying this solution in beams with loss of their structural properties and cross-section, a situation commonly found in historic buildings.

It is noteworthy that the use of partial reinforcement, using mechanical fasteners, in beams with discontinuous geometries do not have analytical modeling to determine their stiffness. This type of study is difficult to experiment with because measurements performed in laboratories describe the behavior of the test only at the measurement points and not continuously. For these elements, the use of analysis by the finite element method allows a global assessment of the reinforcement, enabling a better understanding of the phenomenon studied.

Thus, the present study aimed to analyze the use of steel plate screwed to hardwood beams with cross-section loss. The possibility of recovering the initial stiffness of the element was evaluated, with the main interest in the performance of bolts as mechanical fasteners. Finally, the models were simulated considering the use of carbon fiber mat (CF) as a structural recovery element, and their results compared with the reinforcement with steel plate screwed.

2. MATERIALS AND METHODS

The studied timber beam had a cross-section of 200 x 300 mm with a total length of 6900 mm, supports at a distance of 300 mm from each outer face, meeting the bending test dimensions presented by ABNT NBR 7190 (1997).

The loading aimed to simulate a four-point bending test, according to ASTM D 198 (2015), dimensioned to meet the maximum displacement in the Service Limit State (SLS) of 31.5 mm, according to ABNT NBR 7190 (1997). Thus, equivalent displacements were imposed at the points of application of forces with an intensity of 27.39 mm.

In the parametric study of the models with steel plate screwed, linear analyses were performed using the Abaqus/CAE software, varying the following parameters: timber strength class, quantity, and diameter of bolts, and depth and location of the defect in the beam. All elements were created as deformable solids. The models with CF were simulated with a variation of depth and location of the defect in the beam, considering a fixed geometry of the reinforcement mat in all analyses.

The results of interest were: the resultant force at the point of application of the displacement and the maximum displacement obtained at the center of the beam. With these results, following ABNT NBR 7190 (1997) (Eq. 1), the moment of inertia (Eq. 2) was determined by the flexural stiffness (Eq. 3) of the sets.

$$E_M = \frac{(F_{50\%} - F_{10\%}) \cdot L^3}{(U_{50\%} - U_{10\%}) \cdot 4 \cdot b \cdot h^3} \quad \text{Eq.1}$$

$$I_x = \left(\overline{I_{x,beam}} + A_{beam} \cdot d_{beam}{}^2\right) + \left(\overline{I_{x,plate}} + A_{plate} \cdot d_{plate}{}^2\right) \quad \text{Eq.2}$$

$$(EI) = E_M \cdot I_x \quad \text{Eq.3}$$

Where, E_M is the bending modulus of elasticity (MPa); $F_{50\%}$ and $F_{10\%}$ denote, respectively, half and tenth of the total force obtained (N); $U_{50\%}$ e $U_{10\%}$ denote, respectively, half and tenth of the maximum displacement of the beam (mm); *b*, *h* e *L* are the measurements of the base and height of the cross-section and the length of the beam, respectively (mm); I_x e $\bar{I}_x$ denote, respectively, the moment of inertia of the set and each isolated element (mm⁴); A is the cross-section area (mm²); d is the difference between the CG of the isolated element and the CG of the set (mm); e (*EI*) denotes the stiffness of the assembly (N.mm²).

2.1. Configuration of the models

The constitution of the beam aimed to meet the criteria presented by ABNT NBR 7190 (1997) for hardwoods, and analyzes were carried out for species of classes C20, C30, C40, and C60. For each strength class, species characterized by other researchers were chosen as follows: Paricá (Almeida et al., 2013), Angelim Araroba (Branco et al., 2014), Envira Branca (Christoforo et al., 2013) e Breu Vermelho (Christoforo et al., 2013), with the respective modulus of elasticity of 7320 MPa, 12167 MPa, 14973 MPa, and 16386 MPa.

It was considered a species representing a C50 class, not foreseen by the Brazilian standard, but considered in this study to obtain average values between classes C40 and C60, being chosen the species Canelão, characterized by Christoforo et al. (2013), with a modulus of elasticity of 15355 MPa.

The wood defects were considered on the lower and upper face of the center of the beam span. The length was 690 mm, and it varied between 45, 90, and 135 mm transversally.

The steel plate was simulated with a modulus of elasticity of 200000 MPa, a thickness of 9.5 mm, a length of 1530 mm, and a width of 200 mm. The bolts considered had diameters of 12.7 mm and 15.9 mm, ranging from 2, 4, and 6 bolts long enough to cross the beam section, with a modulus of elasticity similar to that of the plate.

In order to ensure the greatest possible stuffiness when using this system (Li et al., 2021; Waseem et al., 2022), the spacing between the bolts was determined to meet the minimum presented by the Brazilian standard. A distance from the edge of the plate and the beginning of the defect of 115 mm was adopted. Between the axis of the screws, the adopted distance was 95 mm.

A friction factor of 0.4 (O'Ceallaigh et al., 2020) was considered as the contact between the wood, screws, and steel plate. In the models with FC, a perfect adhesion between the reinforcement and the wood was considered, aiming at the ideal behavior of the epoxy fixing adhesive.

The CF mat was modeled with the same dimensions as the steel plate, with a modulus of elasticity of 240000 MPa (Schober et al., 2015). The blanket was considered fully adhered to the wood, aiming at the ideal behavior of the epoxy fixing adhesive, using a contact element type "tie" in Abaqus software.

For each wood resistance class, it was elaborate: a reference model (M0) was prepared, consisting of the timber beam without the defect and the reinforcement, six models considering the defect and without the reinforcement (with MD prefix), 36 models with steel plate screwed reinforcement (with prefix M), and six models with carbon fiber blanket reinforcement (with prefix MFC). The 245 simulations performed are shown in Table 1.

2.2. Numerical model validation and mesh testing

Each component (beam, plate, and bolt) was validated separately, comparing the displacement results obtained in Abaqus/CAE and with the analytical results, varying the type and size of the mesh. All components were simulated with hexahedral (C3D8R) and tetrahedral (C3D4) meshes, varying the size of the elements.

The beam was simulated with 200, 150, 100, and 50 mm elements. In the test, the difference found between the result of the simulations and the result expected by the analytical equation did not exceed 1.2%, with the best result showing a difference of 1.13%.

Thus, considering the large number of elements due to the size of the beam, the processing time was

Table 1 – Settings of the studied models.
Tabela 1 *– Configurações dos modelos estudados.*

Code	Defect (mm/region)	Reinforcement	Code	Defect (mm/region)	Reinforcement
M1	45/lower		M19	45/lower	
M2	90/lower		M20	90/lower	
M3	135/lower	2 bolts with 12.7 mm diameter	M21	135/lower	2 bolts with 15.9 mm
M4	45/upper		M22	45/upper	diameter
M5	90/upper		M23	90/upper	
M6	135/upper		M24	135/upper	
M7	45/lower		M25	45/lower	
M8	90/lower		M26	90/lower	
M9	135/lower	4 bolts with 12.7 mm diameter	M27	135/lower	4 bolts with 15.9mm
M10	45/upper		M28	45/upper	diameter
M11	90/upper		M29	90/upper	
M12	135/ upper		M30	135/ upper	
M13	45/lower		M31	45/lower	
M14	90/lower		M32	90/lower	
M15	135/lower	6 bolts with 12.7 mm diameter	M33	135/lower	6 bolts with 15.9 mm
M16	45/upper		M34	45/upper	diameter
M17	90/upper		M35	90/upper	
M18	135/upper		M36	135/upper	
MD1	45/lower		MFC1	45/lower	
MD2	90/lower		MFC2	90/lower	
MD3	135/lower	Without reinforcement	MFC3	135/lower	Carbon fiber mat
MD4	45/upper		MFC4	45/upper	
MD5	90/upper		MFC5	90/upper	
MD6	135/upper		MFC6	135/upper	

also evaluated, with a result of 3 minutes and 24 seconds for the fastest processing and 27 minutes and 4 seconds for the longest processing.

Considering the processing results obtained for the beam, a 100 mm hexahedral mesh (C3D8R) was adopted for the continuous regions of the element. In the region where the displacement was applied, where there is contact with the plate, and where there is a discontinuity of the element due to the section variation due to the defect, the mesh adopted was 50 mm. The mesh used in the hole region for fixing the screw was 25 mm.

The plate simulation was performed with 10, 25, and 50 mm elements. All numerical results showed differences below 0.5% in relation to the analytical one, converging from the 25 mm elements. Thus, the hexahedral mesh configuration with 25 mm was chosen. In the hole region, the mesh was refined with 5 mm elements.

The CF mat was simulated with the same settings as the steel plate, obtaining similar results. Thus, a 25 mm hexahedral mesh was used in the reinforcement modeling.

The bolt was validated with 20, 10, and 5 mm elements. It was verified that the use of tetrahedral

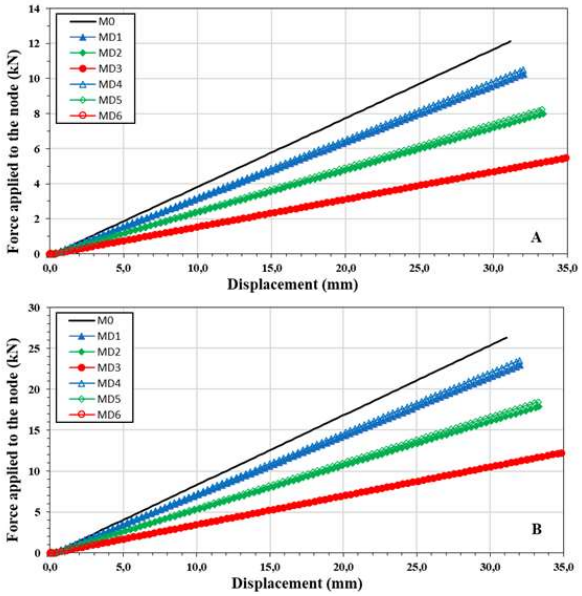

Figure 1 – Models with the defect for strength classes C20 (A) and C60 (B).
Figura 1 *– Modelos com defeito para classes C20 (A) e C60 (B).*

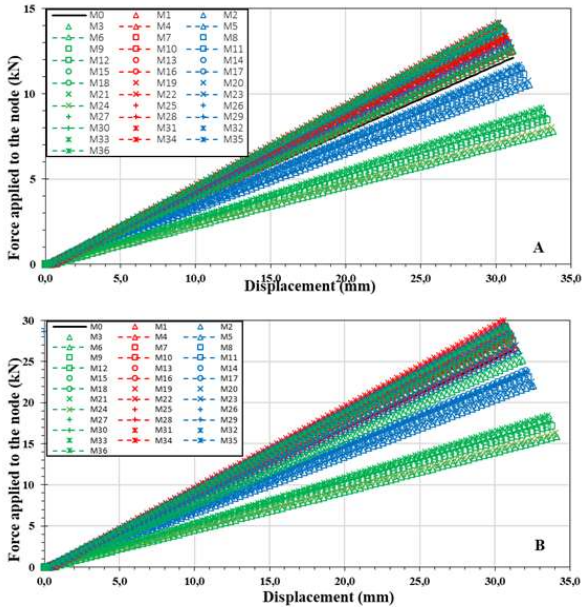

Figure 2 – Models with steel plates screwed for strength C20 (A) and C60 (B).
***Figura 2** – Modelos com chapa de aço parafusada para C20 (A) e C60 (B).*

elements with 20 mm was more efficient, with a bit significant difference in relation to the other sizes of the same geometry in reference to the analytical

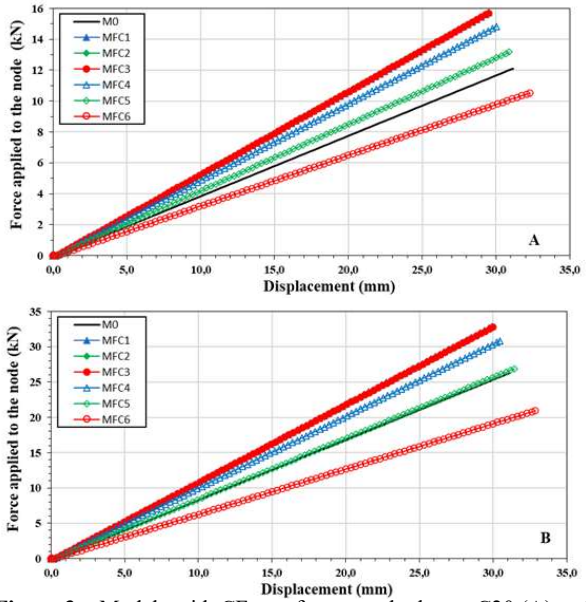

Figure 3 – Models with CF mat for strength classes C20 (A) and C60 (B).
***Figura 3** – Modelos com manta de FC para C20 (A) e C60 (B).*

Note: abscissa axis: the first numeral refers to the number of screws (1p, 2p or 3p); the second refers to the size of the defect (45, 90 or 135); indication of the fault zone ("+" for lower and "- "for higher).
Nota: eixo das abscissas: o primeiro numeral se refere à quantidade de parafusos (1p, 2p ou 3p); o segundo refere-se ao tamanho do defeito (45, 90 ou 135); indicação da zona do defeito ("+" para inferior e "- "para superior).

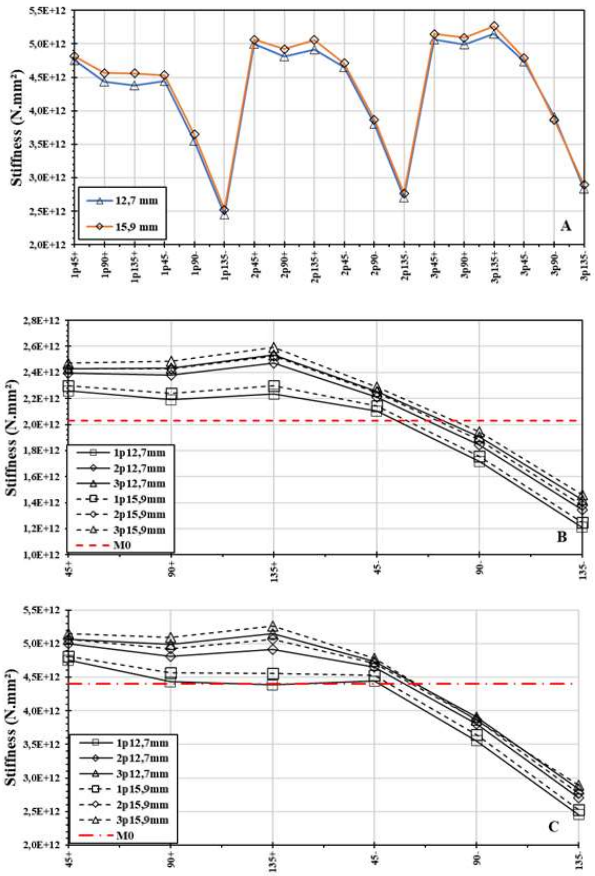

Figure 4 – (a) Rigidity variation with increasing bolt gauge for the class C60; (b) Stuffiness variation with an increasing number of bolts for classes C20; (c) and C60.
***Figura 4** – (a) Variação da rigidez com o aumento da bitola do parafuso para a classe C60; (b) Variação da rigidez com o aumento da quantidade de parafusos para as classes C20; (c) e C60.*

model (2.53%) and with better processing time, being adopted for the continuation of the study. The hexahedral elements showed differences of up to 9.71% in relation to the analytical one.

The simulation was carried out in two processing stages: the initial one, where the model is loaded with its respective boundary conditions, the displacement application, where the load configured incrementally was inserted. The number of increments varied between the 106 and 164 models, with a maximum size of 0.01.

3. RESULTS

Aiming to acknowledge the effect of the loss of cross-section on the stiffness of the beam, the models presented in Table 1 with MD prefix were simulated and compared with the M0 for each strength class. The results were summarized and are shown in Figure 1.

The results of the models with steel plates fixed by bolts, presented in Table 1, were simulated, and their results are presented in Figure 2.

The results of the simulations of the models with carbon fiber reinforcement, with MFC prefix, presented in Table 1 are presented in Figure 3.

The influence of bolts on beam stiffness was studied by varying the diameter and quantity (Table 1). The results presented in Figure 4 were obtained from the models simulated with the C60, which presented the minimum performance in the studies, and figures 4b and 4c present, respectively, the simulated models of the C20 and C60 classes.

4. DISCUSSIONS

The simulations performed with the models predicting only the effects of cross-section loss showed similar behavior in all strength classes (Figure 1). It was observed that the region where the section loss occurs was not a determining factor for the loss of flexural stiffness. In the models with 45 mm of section loss, the stiffness was 14.7% lower than the reference beam. In the models with 90 mm and 135 mm of section loss, the stiffness was, respectively, 36% and 59% lower than the reference.

Classes C40, C50, and C60 presented slight variation between them, with differences between 7% and 9%. The most expressive variations between the other classes were found in the C20 and C30 classes, with 40% and 19%, respectively, in relation to the immediately superior class.

In the simulations of models with steel plate screwed reinforcement (Figure 2), it was observed that the region where the defect is located is relevant to the behavior of the beam, an effect not found without the reinforcement. This occurred because, in the models with the defect located in the tension region, the steel plate located in the lower region of the beam allows obtaining a moment of inertia of the section greater than that found in the models with a defect in the originally compressed area of the section.

All models with a defect height of 135 mm, located in the upper region of the beam, did not achieve the behavior obtained in the reference model. The displacement did not present significant variation in these models, resulting in values approximately 10% higher than the M0. The maximum force found varied between 60% (M6-C60) and 76% (M36-C20) of the reference.

The displacement results were equivalent to the reference in the simulations with a 90 mm height of the defect located in the upper region. The values of maximum force obtained did not reach the result of M0, reaching 11% lower in M11-C60. The models with 45 mm height presented results statistically equivalent to the reference for the same defect region, with slightly superior performance when observing the maximum force obtained.

All simulations performed (Figure 2) with the defect in the lower region of the beam presented results of maximum displacement and maximum force superior to the reference model, resisting a greater load and resulting in a smaller displacement. Similar to what was found in the analysis of the models without reinforcement, the variation in the results obtained for classes C40, C50, and C60 was not very significant.

After obtaining these results, the stiffness restoration capacity of the beam was evaluated. It was possible to observe that all models with defects of 45 mm in both regions and the models with 90 mm and 135 mm of the defect in the lower region presented greater load-bearing capacity than M0. The variation of the timber strength class did not significantly affect the maximum force found in the simulations.

Unlike the behavior observed in the models without reinforcement, where the observed result does not present significant variation when varying the strength class, the models with reinforcement have variation among themselves as the timber class is changed. All the studied models of the C20 class presented a displacement lower than the M0. Except for the models with the greatest defect in the upper region, all the models studied in the C20 class showed a lower displacement than M0. All models with a 135 mm defect in the upper region showed greater displacements than those without reinforcement.

Observing the behavior of each model, it is possible to assess the beneficial behavior that this reinforcement methodology provides to the structural element. Although some models result in higher displacements or lower maximum force, when stiffness is analyzed, all models present better results when compared to their respective models without reinforcement. For all classes, the models with 90 mm and 135 mm defect in the upper region could not restore the stiffness found in M0.

For the positive results, the models with two bolts presented the results closer to the initial model (with a variation of 10%), with better results being found in configurations with more screws (between 11 and 22% higher than the M0).

Compared with the defective and unreinforced models, beneficial effects were observed on the element's stiffness. In models with defects of 45 mm, on both sides of the beam, the increase in stiffness obtained varied between 16% (M4, C60) and 48% (M31, C20).

In the other defect sizes, the difference in location becomes noticeable in the results. For 90 mm defects located in the tensioned region, a variation in stiffness increase between 59% (M2, C60) and 100% (M32, C20) was observed. For defects in the compressed region, the variation was from 23% (M5, C60) to 51% (M35, C20).

In the defects of 135 mm, a stiffness between 34% (M6, C60) and 79% (M36, C20) was found superior to the model without reinforcement for the compressed region and between 140% (M3, C60) and 218% (M33, C20) for the tensioned region. It is observed that, when analyzing all the results, the difference between the models with section loss in different regions becomes greater as the defect size increases.

The participation of timber in the system's rigidity increases as its strength also increases. In this way, the best results were with reinforcement in pieces of timber with lower resistance. No significant differences were found between classes C40, C50, and C60. The loss of cross-section leads to higher stresses acting in the region. It is observed that the models with section loss in the upper region present normal stresses slightly higher than the models with section loss in the lower region.

Evaluating the effect of the reinforcement for these cases, it is observed that the bolts provided the ability to consider a composite cross-section for the beam and the steel plate. Under these conditions, the timber part is subjected to compressive stresses, except for models with a higher strength class and three bolts on each side, where the timber has a region subjected to small tensile stresses.

Compared to the unreinforced sections, the compressive stress to which the section is subjected is considerably lower, reaching 60% of the unreinforced value for the presented M33 models and 85% for the presented M36 models.

When studying the simulations carried out with the models reinforced with CF mat (Figure 3), it was observed that the higher the timber strength class, the greater its contribution to the behavior of the element in service. All defects located in the lower region showed statistically equivalent values. None of the models with a 135 mm defect located in the upper region could recover the support capacity of M0.

Despite the carbon fiber mat being modeled considering a uniformity in the transmission of efforts, the model with the greatest defect in the upper region still did not allow the recovery of the stiffness obtained in M0, reaching a stiffness 24% lower than the reference in the strength class C60. For the studied configurations, the model with the greatest defect in the positive region (MFC3) was the most rigid for all strength classes, with values between 38% (C60) and 46% (C20) higher than M0.

The models with 45 mm and 90 mm in the lower region showed statistically equivalent results, with stiffness approximately 6% lower than the MFC3. The MFC4 Model, of those with section loss in the upper region, was the one that presented greater stuffiness in relation to M0. The model with the closest result to M0 was the MFC5, with stiffness variation between 2% (C60) and 10% (C20) above the initial one.

Models with FC present better results when compared to bolted steel plates. It happens due to the perfect adhesion and, therefore, better transmission of the efforts of the piece of wood to the reinforcing element, as already pointed out by Wassem et al. (2022) e Jasieńko e Nowak (2014).

Although some contribution was identified in the defect simulations in the compressed region, the most

favorable result was a 3% increase in stiffness when comparing 15.9 mm with 12.7 mm bolts. Evaluating the same relationship with the defects in the tensioned region, an increase in stiffness of 10% was found. Similar to the previous analyses, a greater stiffness was observed in the defective elements in the lower region of the beam, where all the simulations were able to reestablish the expected stiffness in M0.

With the increase in the number of bolts, there was also an increase in stiffness in all cases studied. However, the stiffness gain was higher in models with 90 mm and 135 mm of defects in the positive region.

It was identified that the increase in the number of bolts becomes critical for the gain in stiffness with larger defects. When using two bolts on each side, an increase of 7%, 14%, and 29% in stiffness was observed, respectively, for defects of 45 mm, 90 mm, and 135 mm in the tensioned region. When performing the same analysis in the compressed region, values of 6%, 9%, and 14% were found.

Comparing the models with three bolts with those with two screws, gains of 2%, 6%, and 13% were obtained for the pulled region and 2%, 4%, and 7% for the compressed region. Comparing the models with three bolts with one bolt on each side, the results were: 9%, 20%, and 42% increase in stiffness in the tensioned region and 8%, 13%, and 21% for the compressed region.

The variation of the results presented in Figure 4c was similar to that obtained in the C60 class models. However, for the C20 class models, better performance of the reinforcement was observed in these analyses, especially for the models with greater defects in the tensioned region. For these models, there was a greater gain in stiffness when comparing the results of the simulations with two screws on each side with the simulations with one screw on each side. This occurred because the modulus of elasticity of the steel was the same for all simulations and, therefore, the gain in stiffness for beams with woods with a lower modulus of elasticity is of a higher percentage when compared to woods with a higher modulus of elasticity.

5. CONCLUSIONS

According to the results, wood greatly influences flexural stiffness in the models studied. The compressed region of the cross-section was fundamental for recovering the structural capacity of the element in service. For defects located in the compressed region, the studied reinforcement presented less satisfactory results than those obtained for defects in the tensioned region.

Differently from the models with bolted steel plate reinforcement, the simulations with CF mat consider the perfect transmission of forces between the timber beam and the reinforcement element, with better results. The steel plate screwed reinforcement provided stiffness recovery in the same models as the CF mat.

Greater efficiency was observed in the reinforcement with steel plate screwed for the models with lower-strength wood, while the reinforcement with CF mat with epoxy adhesive showed higher relative efficiency for higher timber strength classes.

Changing the diameter of the bolts contributed to the increase in stiffness, reaching a gain of 10% in some models. The efficiency of this solution was higher for defects in the tensioned region. The increase in the number of bolts improved the rigidity of the structural element, reaching 42% higher results when comparing the use of three bolts with one bolt on each side. The increase in stiffness obtained with increasing screw diameter was insignificant for any number of bolts studied.

Regardless of the quantity or diameter of the bolts, all simulated models with defects in the tensioned region and the simulated models with a 45 mm defect in the compressed region were able to overcome the stiffness of the initial model.

AUTHOR CONTRIBUTIONS

P. I. L. G. Jardim contributed to the writing of the paper, numerical simulation and data analysis. F. J. R. Mascarenhas contributed to the writing of the article, translation of the text and data analysis. D. H. de Almeida, A. L. Christoforo and F. A. R. Lahr contributed to the writing of the text and to the analysis and interpretation of the results.

6. REFERENCES

Almeida, D. H. de, Scaliante, R. de M., Macedo, L. B. de, Macêdo, A. N., Dias, A. A., Christoforo,

A. L., & Calil Junior, C. (2013). Caracterização completa da madeira da espécie amazônica Paricá (Schizolobium amazonicum Herb) em peças de dimensões estruturais. *Revista Árvore*, 37(6), 1175–1181. https://doi.org/10.1590/S0100-67622013000600019

American Society for Testing and Materials. (2015). ASTM D 198: *Standard test metholds of static tests of lumber in structural sizes*. ASTM. https://doi.org/10.1520/D0198-15

Associação Brasileira de Normas Técnicas. (1997). NBR 7190: *projetos de estruturas em madeira*. ABNT.

Branco, L. A. M. N., Chahud, E., Christoforo, A. L., Rocco Lahr, F. A., Battistelle, R. A. G., & Valarelli, I. D. (2014). Influence of moisture content in some mechanical properties of two Brazilian tropical wood species. *Advanced Materials Research*, 1025–1026, 42–45. https://doi.org/10.4028/www.scientific.net/AMR.1025-1026.42

Burdzik, W. M. G., & Skorpen, S. (2016). Experimental and analytical investigation into the stiffness of composite steel-reinforced timber beams with flexible shear connectors. *Journal of the South African Institution of Civil Engineering*, 58(4), 11–20. https://doi.org/10.17159/2309-8775/2016/V58N4A2

Christoforo, A. L., Anéris Blecha, K., Luis, A., De Carvalho, C., Fernando, L., Rezende, S., Antonio, F., & Lahr, R. (2013). Characterization of Tropical Wood Species for Use in Civil Constructions. *Journal of Civil Engineering Research*, 2013(3), 98–103. https://doi.org/10.5923/j.jce.20130303.02

Guevara, J. L., Toirac, Y. A., & Marisy, C. M. C. (2019). An approach to the convent of Santa Clara de Asís in Havana. Study of its conservation status and intervention proposals. *Revista ALCONPAT*, 9(2), 228–246. https://doi.org/10.21041/ra.v9i2.354

Jasieńko, J., & Nowak, T. P. (2014). Solid timber beams strengthened with steel plates - Experimental studies. *Construction and Building Materials*, 63, 81–88. https://doi.org/10.1016/j.conbuildmat.2014.04.020

Li, G., Liu, Z., Tang, W., He, D., & Shan, W. (2021). Experimental and Numerical Study on the Flexural Performance of Assembled Steel-Wood Composite Slab. *Sustainability* 2021, Vol. 13, Page 3814, 13(7), 3814. https://doi.org/10.3390/SU13073814

Lukin, M., Prusov, E., Roshchina, S., Karelina, M., & Vatin, N. (2021). Multi-Span composite timber beams with rational steel reinforcements. *Buildings*, 11(2), 1–12. https://doi.org/10.3390/buildings11020046

Martins, J. F. A., & Fioriti, C. F. (2016). Avaliação de manifestações patológicas identificadas nas estruturas em madeira do centro de eventos IBC (Instituto Brasileiro do Café). *REEC - Revista Eletrônica de Engenharia Civil*, 12(3), 43–55. https://doi.org/10.5216/reec.v12i3.39267

O'Ceallaigh, C., Sikora, K., McPolin, D., & Harte, A. M. (2020). Modeling the hygro-mechanical creep behaviour of FRP reinforced timber elements. *Construction and Building Materials*, 259. https://doi.org/10.1016/j.conbuildmat.2020.119899

Schober, K. U., Harte, A. M., Kliger, R., Jockwer, R., Xu, Q., & Chen, J. F. (2015). FRP reinforcement of timber structures. *Construction and Building Materials*, 97, 106–118. https://doi.org/10.1016/j.conbuildmat.2015.06.020

Waseem, S. A., Manzoor, Z., & Bhat, J. A. (2022). An Experimental Investigation into the Behavior of Steel-Timber Composite Beams. *Practice Periodical on Structural Design and Construction*, 27(1), 04021055. https://doi.org/10.1061/(asce)sc.1943-5576.0000636